

DRUG DEVELOPMENT

An oral antisense oligonucleotide for PCSK9 inhibition

Peter Gennemark^{1,2*}, Katrin Walter³, Niclas Clemmensen⁴, Dinko Rekić⁵, Catarina A.M. Nilsson⁵, Jane Knöchel⁵, Mikko Hölttä⁵, Linda Wernevik⁶, Birgitta Rosengren⁷, Dorota Kakol-Palm⁷, Yanfeng Wang⁸, Rosie Z. Yu⁸, Richard S. Geary⁸, Stan J. Riney⁸, Brett P. Monia⁸, Rikard Isaksson⁹, Rasmus Jansson-Löfmark¹, Cristina S. J. Rocha¹⁰, Daniel Lindén⁷, Eva Hurt-Camejo¹¹, Rosanne Crooke⁸, Lloyd Tillman⁸, Tina Rydén-Bergsten⁶, Björn Carlsson⁶, Ulf Andersson¹², Marie Elebring¹, Anna Tivesten¹³, Nigel Davies⁴

Copyright © 2021
The Authors, some
rights reserved;
exclusive licensee
American Association
for the Advancement
of Science. No claim
to original U.S.
Government Works

Inhibitors of proprotein convertase subtilisin/kexin type 9 (PCSK9) reduce low-density lipoprotein (LDL) cholesterol and are used for treatment of dyslipidemia. Current PCSK9 inhibitors are administered via subcutaneous injection. We present a highly potent, chemically modified PCSK9 antisense oligonucleotide (ASO) with potential for oral delivery. Past attempts at oral delivery using earlier-generation ASO chemistries and transient permeation enhancers provided encouraging data, suggesting that improving potency of the ASO could make oral delivery a reality. The constrained ethyl chemistry and liver targeting enabled by *N*-acetylgalactosamine conjugation make this ASO highly potent. A single subcutaneous dose of 90 mg reduced PCSK9 by >90% in humans with elevated LDL cholesterol and a monthly subcutaneous dose of around 25 mg is predicted to reduce PCSK9 by 80% at steady state. To investigate the feasibility of oral administration, the ASO was coformulated in a tablet with sodium caprate as permeation enhancer. Repeated oral daily dosing in dogs resulted in a bioavailability of 7% in the liver (target organ), about fivefold greater than the plasma bioavailability. Target engagement after oral administration was confirmed by intrajejunal administration of a rat-specific surrogate ASO in solution with the enhancer to rats and by plasma PCSK9 and LDL cholesterol lowering in cynomolgus monkey after tablet administration. On the basis of an assumption of 5% liver bioavailability after oral administration in humans, a daily dose of 15 mg is predicted to reduce circulating PCSK9 by 80% at steady state, supporting the development of the compound for oral administration to treat dyslipidemia.

INTRODUCTION

Proprotein convertase subtilisin/kexin type 9 (PCSK9) is a secreted protein involved in regulating hepatic low-density lipoprotein (LDL) receptor life cycle. PCSK9 binds to the extracellular domain of the LDL receptor, targeting the receptor for endosomal degradation rather than recycling to the surface of the hepatocyte after internalization of LDL particles (1). PCSK9 human gain-of-function mutations are linked to familial dominant hypercholesterolemia and loss-of-function mutations result in low concentrations of LDL cholesterol and protect against coronary artery disease (2, 3). This strong human

genetic validation has made PCSK9 inhibition an attractive target therapy for the treatment of atherosclerotic cardiovascular disease.

Inhibition of circulating PCSK9 by use of monoclonal antibodies (mAbs) reduces LDL cholesterol and demonstrated an outcome benefit in patients with cardiovascular disease (4–6). In addition, a gene silencing therapeutic approach to inhibit PCSK9 mRNA by small interfering RNA (siRNA) has recently been filed for marketing approval and showed substantial lowering of plasma LDL cholesterol (7–9). Yet, these current therapeutic PCSK9 inhibitors require administration by injection (10). An oral PCSK9 inhibitor would offer patients an alternative, more convenient, route of administration.

We present AZD8233 (also known as ION-863633), a highly potent 16-nucleotide oligomer triantennary *N*-acetylgalactosamine (GalNAc) antisense oligonucleotide (ASO) with constrained ethyl (cEt) chemistry that is designed to target PCSK9 mRNA, thereby inhibiting the intracellular protein translation and synthesis of PCSK9 protein. The GalNAc chemistry promotes liver uptake via the asialoglycoprotein (ASGP) receptor primarily expressed on hepatocytes, resulting in 10- to 30-fold increased potency in isolated hepatocytes, in vivo animal models (11–13) and in the clinic (13, 14). The half-life of ASOs in the liver is in the order of weeks (15). We reasoned that the high potency of AZD8233, together with a long liver half-life, could make once daily oral administration of interest to explore.

Oral delivery of ASOs is challenging because they are highly charged, hydrophilic macromolecules, with inherently poor intestinal permeability and, hence, are expected to have negligible systemic bioavailability after this route of administration. To address this issue, earlier generations of ASOs were formulated with permeability enhancers such as sodium caprate to transiently and reversibly alter membrane permeability (16, 17). The combination of ASO formulated

¹Drug Metabolism and Pharmacokinetics, Research and Early Development, Cardiovascular, Renal, and Metabolism (CVRM), BioPharmaceuticals R&D, AstraZeneca, SE-431 50 Gothenburg, Sweden. ²Department of Biomedical Engineering, Linköping University, SE-581 83 Linköping, Sweden. ³Inhalation Product Development, Pharmaceutical Technology and Development, Operations, AstraZeneca, SE-431 50 Gothenburg, Sweden. ⁴Advanced Drug Delivery, Pharmaceutical Sciences, R&D, AstraZeneca, SE-431 50 Gothenburg, Sweden. ⁵Clinical Pharmacology and Quantitative Pharmacology, Clinical Pharmacology and Safety Sciences, BioPharmaceuticals R&D, AstraZeneca, SE-431 50 Gothenburg, Sweden. ⁶Research and Early Development, Cardiovascular, Renal, and Metabolism (CVRM), BioPharmaceuticals R&D, AstraZeneca, SE-431 50 Gothenburg, Sweden. ⁷Bioscience Metabolism, Research and Early Development, Cardiovascular, Renal, and Metabolism (CVRM), BioPharmaceuticals R&D, AstraZeneca, SE-431 50 Gothenburg, Sweden. ⁸Ionis Pharmaceuticals Inc., 2855 Gazelle Court, Carlsbad, CA 92010, USA. ⁹Early Biometrics and Statistical Innovation, Data Science and Artificial Intelligence, BioPharmaceuticals R&D, AstraZeneca, SE-431 50 Gothenburg, Sweden. ¹⁰Functional and Mechanistic Safety, Clinical Pharmacology and Safety Sciences, R&D, AstraZeneca, SE-431 50 Gothenburg, Sweden. ¹¹Translational Science and Experimental Medicine, Research and Early Development, Cardiovascular, Renal, and Metabolism (CVRM), BioPharmaceuticals R&D, AstraZeneca, SE-431 50 Gothenburg, Sweden. ¹²CVRM Safety, Clinical Pharmacology and Safety Sciences, BioPharmaceuticals R&D, AstraZeneca, SE-431 50 Gothenburg, Sweden. ¹³CVRM CMC Projects, Pharmaceutical Sciences, R&D, AstraZeneca, SE-431 50 Gothenburg, Sweden.

*Corresponding author. Email: peter.gennemark@astrazeneca.com

with sodium caprate was previously reported to result in systemic ASO bioavailability of about 10% in humans (18). However, despite a reasonable bioavailability, the doses of the ASO with the 2'-O-(2-methoxyethyl) chemistry were high, requiring administration of multiple units and gram quantities of sodium caprate. With the high potency of AZD8233 and, hence, a low dose, we hypothesized that oral delivery could be feasible using amounts of sodium caprate that could reasonably be formulated into a single-unit, enteric-coated tablet. Furthermore, we hypothesized that oral dosing would improve ASO drug delivery to hepatocytes, the target tissue, taking full advantage of the "first-pass extraction effect" by the liver after intestinal absorption and minimize the exposure to extrahepatic organs/tissues.

This study presents the discovery and pharmacokinetic (PK) and pharmacodynamic (PD) characterization of AZD8233 after subcutaneous (SC) administration, demonstrating its high potency in both animals and humans. In addition, we explored the feasibility of oral administration of AZD8233 in a series of experiments in rat, dog, and monkey. The data support the development of AZD8233 as an oral dosage form and indicate potential for oral delivery of ASOs in general. Formally, AZD8233 is referred to as AZD6615 when formulated as an oral dosage form. However, to simplify terminology, the name AZD8233 and administration route are used throughout this paper.

RESULTS

Discovery of AZD8233 and potency in PCSK9 transgenic mice

AZD8233 was selected on the basis of extensive cell culture, rodent, and cynomolgus monkey screens to identify the most potent, most selective, and best-tolerated ASO for suppressing PCSK9 mRNA expression in the liver and plasma concentrations of PCSK9 protein. It is a 16-base cEt phosphorothioate-modified ASO that is conjugated at its 5' end to a triantennary GalNAc (fig. S1 and table S1). Further, it is a 3-10-3 gapmer, containing three cEt-modified ribonucleotides in each end and 2'-deoxynucleotides in the middle portion of the molecule. AZD8233 without the GalNAc moiety, i.e., the parent drug, is referred to as nonconjugated AZD8233 (also known as ION-848833). After administration of AZD8233, the GalNAc will be cleaved after hepatocyte uptake in the liver. Measured liver concentrations [liquid chromatography with tandem mass spectrometry (LC-MS/MS)], hence, correspond to unconjugated AZD8233, whereas measured plasma concentrations (hybridization electrochemiluminescence) correspond to the sum of unconjugated and conjugated ASO. Note that liver concentration reflects liver homogenate concentration and not hepatocyte concentration.

Potency was assessed by weekly subcutaneous injections of AZD8233 in transgenic mice overexpressing human PCSK9 in a 4-week study. AZD8233 liver exposure increased dose dependently (Fig. 1A), with concomitant dose-dependent reduction of human plasma PCSK9 and LDL cholesterol (Fig. 1, B and C). Liver exposure of 4 µg/g (3 and 5 µg/g; 5th and 95th percentiles) was predicted to result in 80% reduction in plasma PCSK9 (Fig. 1D). This liver concentration was used as the target concentration in subsequent PK studies and for human PKPD simulations. In line with previous experience in preclinical (11–13) and clinical models (13, 14), administration of AZD8233 demonstrated about 10-fold increase in potency compared to administration of the nonconjugated parent ASO: Doses of AZD8233 (0.5 mg/kg) (Fig. 1B) and nonconjugated parent (5 mg/kg) (fig. S2) were required to reduce PCSK9 by 80%, and liver exposures predicted to result in 80% reduction in plasma PCSK9 were 4 µg/g for AZD8233 (Fig. 1D) and 39 µg/g for the nonconjugated parent (fig. S2).

Lipoprotein lipid composition in wild-type mice after Pcsk9 GalNAc ASO treatment

The extent to which a GalNAc ASO targeting the PCSK9 transcript can reduce relevant dyslipidemia biomarkers was next investigated in wild-type mice after subcutaneous administration. A mouse surrogate Pcsk9 GalNAc ASO (ION-866672, administered 5 mg/kg SC once weekly

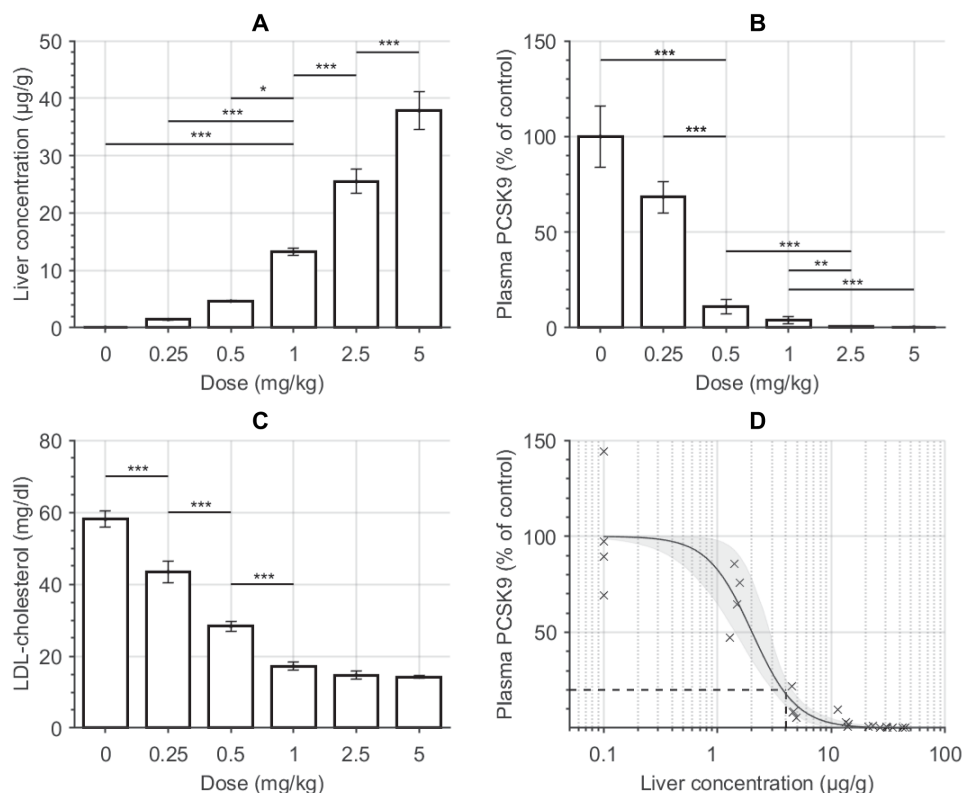


Fig. 1. Four-week dose-response study with once weekly subcutaneous administration of AZD8233 in transgenic mice overexpressing human PCSK9. (A) Liver exposure at termination increases with dose. (B and C) AZD8233 dose-dependently reduced human plasma PCSK9 (B) and LDL cholesterol (C). (D) Plasma PCSK9 versus liver exposure (crosses), and model fit (solid line) with gray shaded area indicating the 5th and 95th percentiles of the point prediction. Liver exposure of 4 µg/g resulted in 80% reduction of PCSK9 (dashed lines). The study included six dose groups, with $N = 4$ mice per group. In (A) to (C), error bars denote SEM, and the horizontal bars indicate the significant differences between treatments (* $P < 0.05$, ** $P < 0.01$, and *** $P < 0.005$) for Tukey's post hoc test.

for 6 weeks) targeting endogenous mouse *Pcsk9* transcript potentially reduced plasma mouse PCSK9 protein concentrations by 97% compared to vehicle control, indicating that most of the circulating pool of PCSK9 is derived from production in the liver (table S2). The PCSK9 protein reduction was associated with 176% increased liver Ldlr protein expression in lean chow-fed mice (table S2). Knocking down mouse *Pcsk9* with the *Pcsk9* ASO reduced plasma total cholesterol (–29%), LDL cholesterol (–67%), high-density lipoprotein (HDL) cholesterol (–31%), LDL triglyceride (–75%), LDL phospholipid (–72%), and HDL phospholipid (–31%) concentrations (table S2). The total lipid (cholesterol, triglyceride, and phospholipid)-to-protein ratio was reduced in HDL particles while the ratio was unchanged in very LDL (VLDL), intermediate-density lipoprotein (IDL), and LDL particles after *Pcsk9* ASO treatment, demonstrating reduced HDL but not VLDL, IDL, or LDL particle size (table S2). There was no effect on VLDL lipid particle composition, indicating no effect on VLDL secretion (table S2). *Pcsk9* GalNAc ASO treatment did not reduce in vivo VLDL triglyceride secretion in a separate experiment using Triton WR1339 to block lipase activity (fig. S3). These studies demonstrated that targeting endogenous liver *Pcsk9* expression with a GalNAc-ASO approach is a powerful strategy to ablate circulating PCSK9, induce hepatic Ldlr expression, and thereby reduce plasma total and LDL cholesterol concentrations.

Liver half-life of unconjugated AZD8233 in cynomolgus monkey and liver exposure for GalNAc-conjugated ASOs

The PK of AZD8233 was investigated in cynomolgus monkeys with four monthly subcutaneous injections (2, 8, or 32 mg/kg) and one extra loading dose 1 week after the first dose. AZD8233 demonstrated nonlinear PK, with maximum liver concentration increasing less than proportionally with dose (Fig. 2). To estimate tissue half-life, one satellite group (8 mg/kg) was dosed only on day 1, and another satellite group (32 mg/kg) was continued with a 3-month washout after the last dose before termination. The liver exposure half-life was estimated to be 17.6 days (15 and 21 days; 5th and 95th percentiles) based on mathematical modeling, taking all liver exposure data

simultaneously into account (Fig. 2). The magnitude and half-life of unconjugated AZD8233 liver exposure in cynomolgus monkeys compared reasonably well with previously reported data on a GalNAc-conjugated 2'-O-(2-methoxyethyl) ASO for relevant dose levels (Fig. 2) (15). Overall, these data confirm that unconjugated AZD8233 has a liver half-life in the order of weeks and that liver exposure of AZD8233 is at expected concentrations previously described for GalNAc-conjugated ASOs in cynomolgus monkey.

Circulating PCSK9 in humans after subcutaneous administration of AZD8233

Single subcutaneous doses (12, 30, and 90 mg) of AZD8233 potentially and dose-dependently reduced plasma PCSK9 protein concentrations in humans with a baseline LDL cholesterol of 134 ± 3.9 mg/dl (means \pm SEM) (Fig. 3). For the 90-mg dose, circulating PCSK9 was reduced by up to 95% and remained reduced to more than 90% over at least 1 month (Fig. 3, A and B). The corresponding maximal mean reduction in LDL cholesterol was 68% for the 90-mg dose group (Fig. 3, C and D). Both PCSK9 and LDL cholesterol slowly returned to baseline or close to baseline over the 16 weeks after dose follow-up period.

Liver bioavailability and reduction of hepatic target mRNA in rats upon intrajejunal administration

To study the potential of AZD8233 for oral delivery, the liver bioavailability in jejunal cannulated rats was quantified using both intrajejunal (IJ) and subcutaneous single-dose administration (I) doses of 3, 10, 20, and 40 mg/kg together with sodium carprate at 300 mg/kg as permeation enhancer; subcutaneous doses of 0.3, 1, 2, and 4 mg/kg without permeation enhancer). This in vivo model with the IJ route of administration is intended to mimic oral administration of tablets, which is not feasible in rodents. At the desired liver concentration of 4 μ g/g, predicted to result in 80% PCSK9 reduction based on transgenic mouse data, the liver bioavailability of IJ compared to subcutaneous administration of AZD8233 was 5.3% (4.2 and 6.2%; 5th and 95th percentiles) (Fig. 4A).

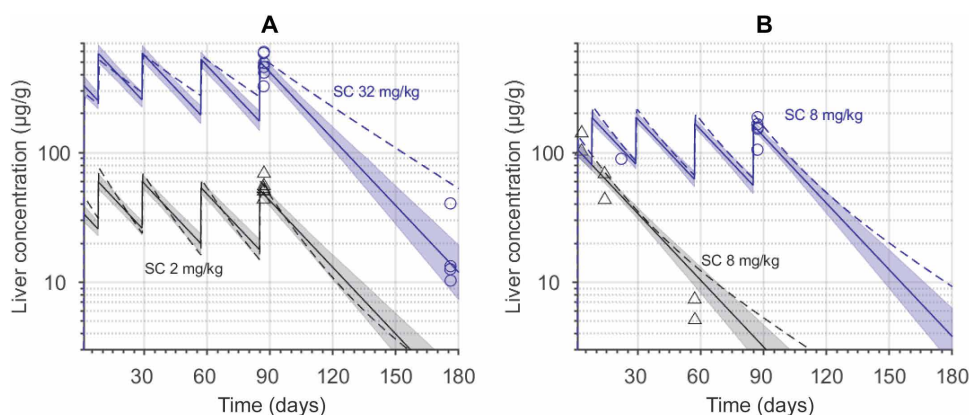


Fig. 2. Liver concentration–time profiles of unconjugated AZD8233 in cynomolgus monkeys. (A) Liver concentration after repeated subcutaneous once monthly dosing of 2 mg/kg ($N = 6$) and 32 mg/kg ($N = 10$) of AZD8233. (B) Liver concentration after single subcutaneous dosing and repeated subcutaneous once monthly dosing of 8 mg/kg ($N = 12$) of AZD8233. The markers indicate the observed data at termination. The solid lines represent a prediction based on a nonlinear one-compartment PK model simultaneously fitted to data from all groups. The shaded areas indicate the 5th and 95th percentiles of the point prediction. The dashed lines show the simulations of the Yu *et al.* (15) literature model [ION-681257, a GalNAc-conjugated 2'-O-(2-methoxyethyl) ASO].

Because AZD8233 is not active in rodents, a rat-specific GalNAc-conjugated *Malat-1* ASO (GalNAc3-conjugate 3-10-3 cEt gapmer targeting *Malat-1*; ION-704361) with the same chemistry as AZD8233 was used to confirm target engagement in the form of mRNA knock-down after IJ administration. Again, at the desired liver exposure of 4 μ g/g, the liver bioavailability of IJ compared to subcutaneous administration was 5.0% (4.3 and 5.9%) for the rat-specific ASO (Fig. 4B). The rat-specific ASO and AZD8233 displayed highly similar dose to liver exposure relationships both for subcutaneous and IJ administration, and consequently, the bioavailability was also similar (Fig. 4, A and B). Hence, the rat-specific *Malat-1* ASO is representative of AZD8233 with respect to liver exposure and bioavailability.

The average liver mRNA concentration of *Malat-1* was reduced to ≥ 73 and $\geq 78\%$ in all dosed subcutaneous and IJ groups,

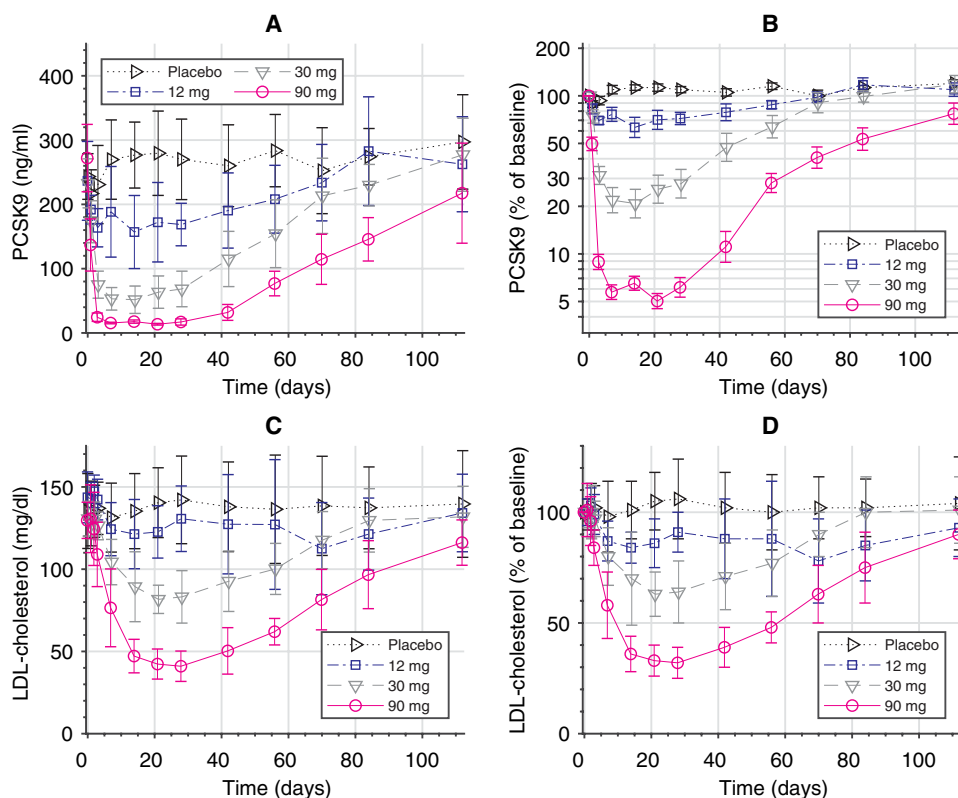


Fig. 3. Plasma PCSK9 concentrations upon single subcutaneous dosing of AZD8233 to humans with elevated LDL cholesterol concentrations. (A and B) Circulating PCSK9 in the form of measured data (A) and baseline-corrected data at logarithmic scale for improved resolution (B). (C and D) Circulating LDL cholesterol in the form of measured data (C) and baseline-corrected data (D). $N = 6$ per treated group and $N = 14$ for placebo. Error bars denote SEM.

respectively (Fig. 4C). The productive bioavailability, reflecting target cell bioavailability and measured indirectly by target engagement, of IJ compared to subcutaneous was estimated to be 29% (10 and 100%; 5th and 95th percentiles) at 80% *Malat-1* knockdown (Fig. 4D). The discrepancy between bioavailability measured from exposure in total liver, including all cell types, and productive bioavailability may be a result of the ASGP receptor being expressed only on hepatocytes, believed to be the target cell population. A separate study in the same animal model demonstrated that the rat-specific GalNAc-conjugated *Malat-1* ASO does not reduce *Malat-1* mRNA in the intestine after IJ administration (table S3).

Liver bioavailability in dogs after once daily administration of AZD8233 tablets

Plasma and liver exposure was measured upon daily oral dosing of a tablet containing 700-mg sodium caprate formulated with either 3 or 20 mg of AZD8233 for 7 or 28 days in beagle dogs. Once daily subcutaneous administration of 1 mg was used as control. The exposure in terms of maximum plasma concentration (C_{max}) and area under the plasma concentration time curve (AUC) increased approximately in proportion to the dose of AZD8233 between 3 and 20 mg/day on days 1, 7, and 28 (Fig. 5A and fig. S4). The plasma bioavailability was 1 to 2% (Table 1).

Unconjugated AZD8233 accumulated in the liver over time (Fig. 5B). Liver bioavailability of 7% was about fivefold greater than the plasma bioavailability (Table 1). Selective uptake by the liver is

further supported by the limited kidney bioavailability of 1 to 2%, in the same range as plasma bioavailability (Table 1).

A potential difference between the oral and the subcutaneous route of administration could be the knockdown of PCSK9 in the gut as PCSK9 is expressed in the intestine (19). However, all but one jejunum sample had exposures below the limit of quantification of the ASO, hence $<0.5 \mu\text{g/g}$ (the exception was the jejunum sample from one dog in the 20 mg/day oral group that had $0.54 \mu\text{g/g}$ at day 7). At such low exposure, virtually, no PCSK9 knockdown in the jejunum is expected on the basis of the knockdown-to-tissue concentration relationship.

AZD8233 liver exposure could be represented by a linear one-compartment model (Fig. 5B), with estimated uptake rate of 24.5 day^{-1} (15 and 38 day^{-1} ; 5th and 95th percentiles), volume of distribution of 0.0631 liter/kg (0.039 and 0.091 liter/kg), elimination rate constant of 0.0590 day^{-1} (0.018 and 0.12 day^{-1}), and bioavailability of 0.0690 (0.052 and 0.091). Because a linear model sufficed to represent data, the modeling confirms that liver PK is in a linear range at therapeutically relevant concentrations. The model-predicted liver half-life was 11.8 days (5.8 and 38 days). The estimated volume of distribution for the liver PK model is relatively low at

0.06 liter/kg , suggesting that most of the absorbed ASO distributes to the liver because the physiological volume of a dog liver is about 0.05 liter/kg (20). In all cases, AZD8233 was well tolerated after daily dosing to male beagle dogs for up to 28 days at 3 or 20 mg/day (oral tablets) or at 1 mg/day (SC) except mild inflammatory reactions at the injection site.

LDL cholesterol in healthy monkeys after oral and subcutaneous administration of AZD8233

The tolerability of high doses of AZD8233 tablets (28, 42, and 56 mg/day) in healthy cynomolgus monkeys after daily oral administration was investigated in a 14-day study. Average predose concentrations of plasma PCSK9 were in the range 180 to 380 ng/ml for all animals. After 7 days of dosing, there was a marked decrease in PCSK9 of greater than 50% in all dose groups, and overall, the decrease was more pronounced at the end of the study, albeit not dose dependent (Fig. 6A). For the two lower doses, almost complete inhibition was observed at day 14. Liver exposure at termination day 14 was also independent of dose with an average of $46 \pm 6 \mu\text{g/g}$ (means \pm SEM) (table S4), being one order of magnitude greater than the liver exposure required for 80% reduction of PCSK9 in the transgenic mouse. The magnitude of PCSK9 reduction is therefore generally consistent with the observed high liver exposure, as predicted by the liver-to-PCSK9 relationship obtained in the transgenic mouse.

For plasma LDL cholesterol, the average predose concentration was $55 \pm 2.7 \text{ mg/dl}$ (means \pm SEM), and the concentration was reduced by 45 to 50% at day 14 (Fig. 6B). Note that this is likely an

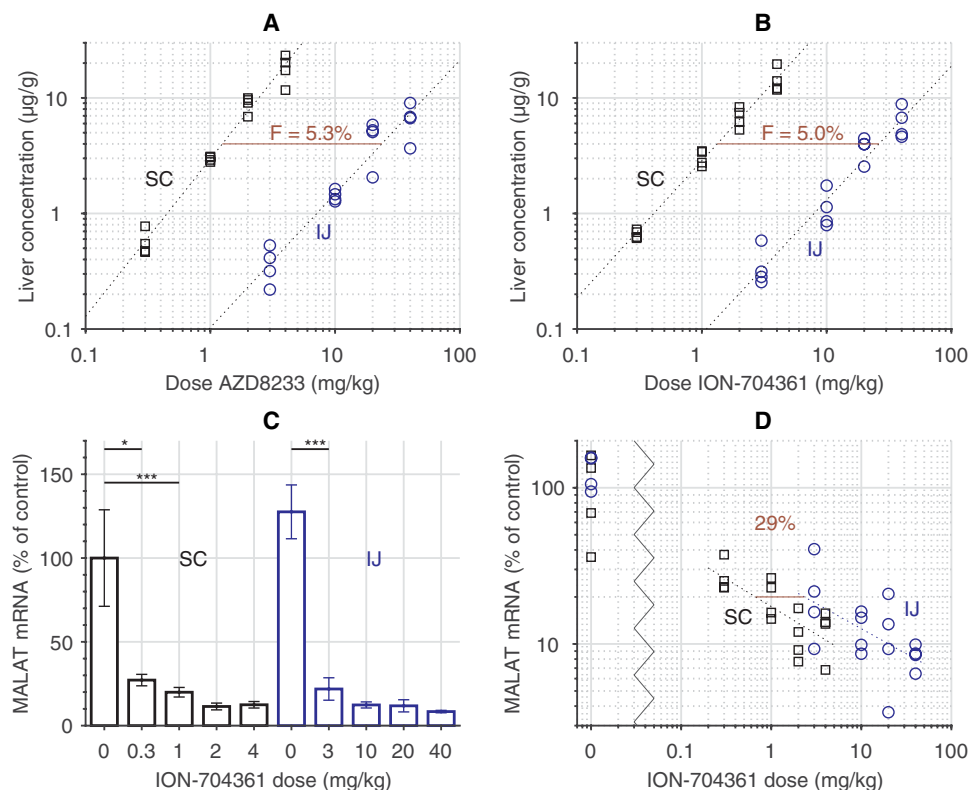


Fig. 4. Single dose of AZD8233 or rat-specific tool ASO targeting Malat-1 (ION-704361) after subcutaneous or IJ administration to rats. (A) Liver concentration of unconjugated AZD8233 48 hours after dose versus dose of AZD8233. (B) Liver concentration of unconjugated ION-704361 48 hours after dose versus dose of ION-704361. In (A) and (B), the dotted lines represent a linear regression of data for respective administration route and compound. The liver bioavailability (F) of IJ compared to subcutaneous is indicated in red at the desired liver exposure of 4 µg/g. (C) *Malat-1* mRNA expression (relative to the subcutaneous control group that is normalized to 100%) in the liver versus ION-704361 dose for subcutaneous and IJ administration. Error bars denote SEM, and the horizontal bars indicate the significant differences between treatments ($*P < 0.05$ and $***P < 0.005$) for Tukey's post hoc test. (D) Individual data from (C) plotted versus dose. The dotted lines represent a linear regression of data for respective administration route and compound. The productive bioavailability of IJ compared to subcutaneous at the desired liver exposure of 4 µg/g was 29%. The x axis is broken to allow the control groups at dose 0 to be included. The study included five dose groups per route of administration, with $N = 4$ rats per group.

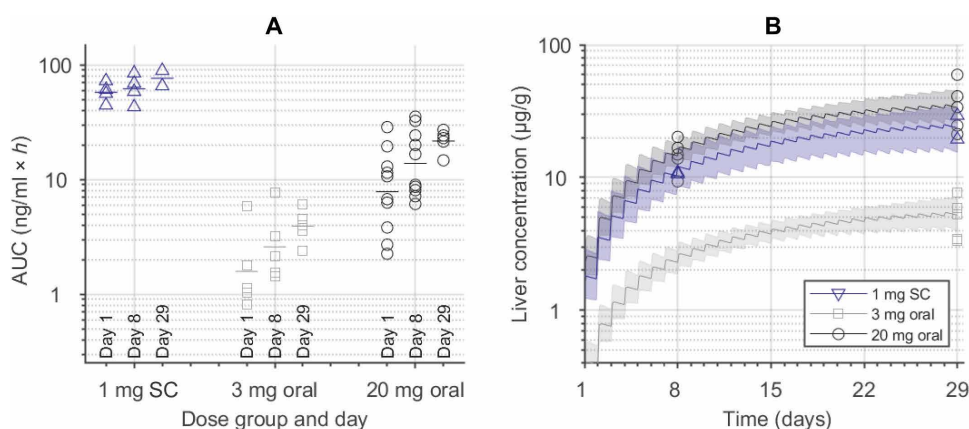


Fig. 5. Repeated daily oral administration of AZD8233 tablets to dogs. (A) Estimated areas under the curve (AUCs) of the plasma exposure data. The geometric means are indicated by horizontal lines. (B) Unconjugated AZD8233 liver exposure time courses. The solid lines represent a one-compartmental mathematical model fit to all data simultaneously, and the shaded areas indicate the 5th and 95th percentiles of the point prediction. The study included three dose groups, with $N = 4$ for the subcutaneous group, $N = 5$ for the 3 mg/day oral group, and $N = 10$ for the 20 mg/day oral group.

underestimate of the PD effect as the system is not in a steady state because the liver half-life of 18 days is greater than the study duration. The LDL cholesterol reduction was again independent of dose, reflecting the high doses used in the study. For comparison, the LDL cholesterol reduction after subcutaneous administration of AZD8233 was in the range 59 to 74% after 3 weeks in a more extended 3-month study (Fig. 6C). The subcutaneous study was also conducted in healthy monkeys with an average predose concentration of 52 ± 2.4 mg/dl (means \pm SEM) (Fig. 6C) and again dosed at greater than therapeutically relevant doses. Total cholesterol showed a trend to decrease over the 14 days, for all dose groups, whereas triglycerides did not show any clear trend for the two lowest dose groups, but tended to increase in the high-dose group (table S4).

In all cases, the AZD8233 tablets were well tolerated for 14 days (albeit associated with transient instances of liquid feces). Isolated instances of vomiting were observed immediately after dosing in all animals in the two highest dose groups, receiving three and four enteric-coated tablets daily. The cause of the emesis was considered to be procedural in origin, because there was no evidence of the tablets being present in the vomit.

Prediction of repeated oral dosing of AZD8233 in human

Predicted liver exposure and reductions of PCSK9 and LDL cholesterol in humans after once daily oral AZD8233 treatment (15 mg/day), assuming 5% liver bioavailability, in comparison to once monthly subcutaneous administration (25 mg/month) of AZD8233 are depicted in Fig. 7. The doses were chosen to give 80% PCSK9 reduction at steady state. The estimated liver exposure half-life of about 18 days results in a predicted 26-fold accumulation of liver concentration at steady state for once daily administration, as illustrated by the increase in liver exposure over time in Fig. 7A. Main uncertainties in the human dose prediction for oral administration are the translation of the oral bioavailability. The prediction is conservative in the sense that it does not assume the “productive” bioavailability observed in the rat study, which was greater than the liver bioavailability of 5 to 7% observed in rat and dog.

Table 1. Relative bioavailability of tablets compared to subcutaneous injection in plasma, liver, and kidney in beagle dogs after once daily oral administration. The plasma bioavailability is based on AUC for more than 24 hours, whereas the tissue bioavailability is based on samples taken 24 hours after last dose.

Oral dose (mg/day)	Time (day)	Plasma bioavailability (%; means \pm SEM)	Liver bioavailability (%; means \pm SEM)	Kidney bioavailability (%; means \pm SEM)
3	29	1.8 \pm 0.26	7.0 \pm 1.0	1.6 \pm 0.24
20	8	1.3 \pm 0.28	7.0 \pm 0.74	1.2 \pm 0.13
20	29	1.4 \pm 0.22	7.4 \pm 1.2	1.2 \pm 0.19

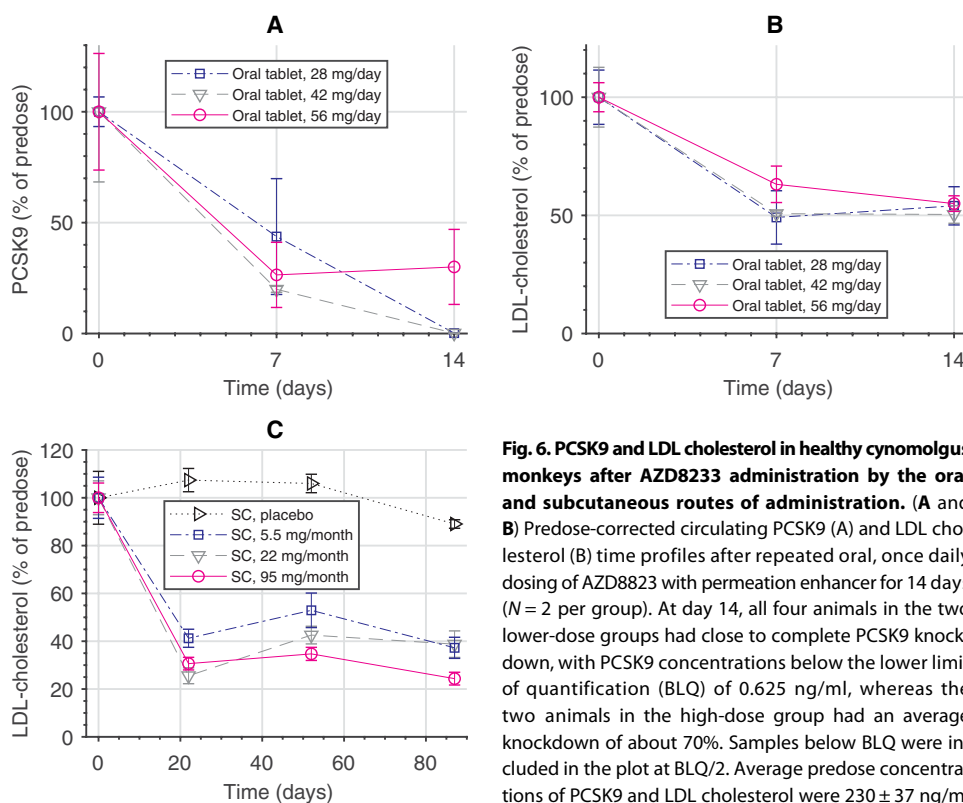


Fig. 6. PCSK9 and LDL cholesterol in healthy cynomolgus monkeys after AZD8233 administration by the oral and subcutaneous routes of administration. (A and B) Predose-corrected circulating PCSK9 (A) and LDL cholesterol (B) time profiles after repeated oral, once daily dosing of AZD8233 with permeation enhancer for 14 days ($N = 2$ per group). At day 14, all four animals in the two lower-dose groups had close to complete PCSK9 knockdown, with PCSK9 concentrations below the lower limit of quantification (BLQ) of 0.625 ng/ml, whereas the two animals in the high-dose group had an average knockdown of about 70%. Samples below BLQ were included in the plot at BLQ/2. Average predose concentrations of PCSK9 and LDL cholesterol were 230 ± 37 ng/ml and 55 ± 2.7 mg/dl (means \pm SEM), respectively. (C) Repeated once monthly subcutaneous dosing of AZD8233 by injection for 3 months ($N = 6$ to 10 per group). Data are relative to the average of two predose values sampled 1 and 2 weeks before the start of treatment. Error bars denote SEM. Average predose concentration of LDL cholesterol was 52 ± 2.4 mg/dl (means \pm SEM).

peated once monthly subcutaneous dosing of AZD8233 by injection for 3 months ($N = 6$ to 10 per group). Data are relative to the average of two predose values sampled 1 and 2 weeks before the start of treatment. Error bars denote SEM. Average predose concentration of LDL cholesterol was 52 ± 2.4 mg/dl (means \pm SEM).

DISCUSSION

Currently available inhibitors of PCSK9 are administered by injection. The development of a PCSK9 inhibitor that could be administered orally would offer patients a convenient and noninvasive alternative, which could possibly lead to improved compliance and better treatment outcomes. Here, we present AZD8233, a potent GalNAc-conjugated ASO for PCSK9 inhibition with potential for oral delivery.

Two important properties of AZD8233 render it feasible for oral administration. First, the potency is high because of the cEt chemistry (21, 22) and the use of GalNAc conjugation resulting in hepatocyte targeting (23). This allows the dose of ASO to be reduced by about two orders of magnitude compared to older generations of chemistry without GalNAc conjugation. This high potency was confirmed by the subcutaneous study in man, where a single

dose of 90 mg sufficed to reduce circulating PCSK9 by >90%. This reduction is similar to that achieved with Abs (24) and greater than the ~80% reduction observed with siRNA (8, 9, 24). Second, the half-life in the liver is 2 to 3 weeks, in agreement with historical data of other ASOs (15, 25), allowing the ASO to accumulate in the liver over time after repeated once daily dosing. This is important because the long tissue half-life and expected accumulation will lead to overlap in liver exposure from consecutive daily dosing, thereby minimizing the impact of day-to-day variability in uptake expected after oral administration (26). Hence, at steady state, the within-day variability in tissue exposure can be expected to be markedly less than the day-to-day variability in uptake typically seen after single oral dosing of ASOs (18). In addition, oral delivery of GalNAc-conjugated ASOs targeting the liver is generally favored by “first-pass extraction” after absorption.

The feasibility for oral administration of AZD8233 was demonstrated in three studies. The first study demonstrated target knockdown capability in the jejunal cannulated rat model after IJ administration of a rat-specific tool ASO. Productive bioavailability as measured by mRNA knockdown was about six times greater than liver bioavailability

for IJ compared to subcutaneous administration at therapeutically relevant doses. This could likely be explained by an active uptake of the GalNAc-conjugated ASO by the liver from the vena porta by the ASGP receptor after oral administration. Because AZD8233 and the tool ASO showed similar liver exposure profiles, it is likely that AZD8233 has similar advantageous target engagement properties upon IJ administration as the tool compound. The second study, conducted in dogs, demonstrated that clinically relevant liver exposures could be achieved after repeated daily oral administration of tablets. The fivefold greater liver bioavailability compared to plasma is again likely a result of active uptake in the liver. The observed low bioavailability of AZD8233 to plasma and kidney (and likely to other tissues) in comparison to liver in the dogs is beneficial because it decreases exposure in organs other than the liver. The third study

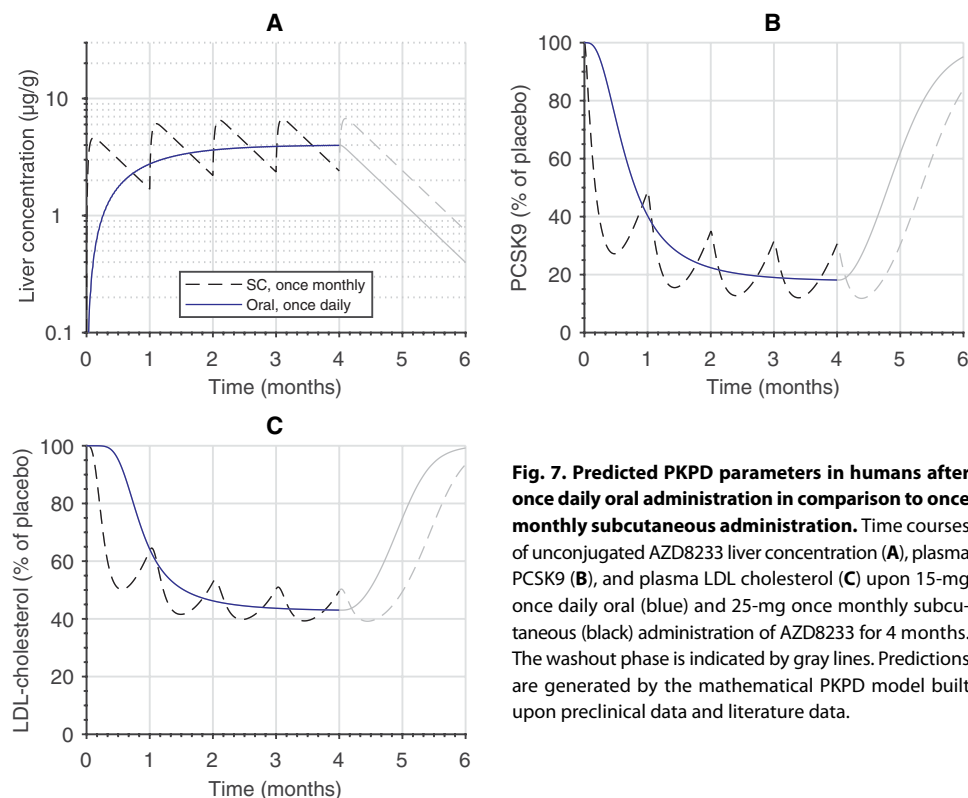


Fig. 7. Predicted PKPD parameters in humans after once daily oral administration in comparison to once monthly subcutaneous administration. Time courses of unconjugated AZD8233 liver concentration (A), plasma PCSK9 (B), and plasma LDL cholesterol (C) upon 15-mg once daily oral (blue) and 25-mg once monthly subcutaneous (black) administration of AZD8233 for 4 months. The washout phase is indicated by gray lines. Predictions are generated by the mathematical PKPD model built upon preclinical data and literature data.

showed target engagement in the form of plasma PCSK9 and LDL cholesterol reduction in cynomolgus monkeys upon repeated oral, once daily administration.

We expect that oral administration of a GalNAc-conjugated PCSK9 ASO to result in similar PD effects as compared to subcutaneous administration. A potential difference could be the knockdown of PCSK9 in the gut, because PCSK9 is expressed in the intestine (19). However, such knockdown is not likely because the proposed leading mechanism of sodium caprate is promotion of paracellular, rather than intracellular, uptake (27), and enhanced cellular uptake from the GalNAc receptor is not expected because it is almost exclusively expressed in hepatocytes (28, 29). Furthermore, presented dog data show jejunum concentrations of AZD8233 below the limit of quantification, not expected to cause PCSK9 knockdown, and the rat-specific *Malat-1* ASO demonstrated no knockdown of *Malat-1* mRNA in jejunum after IJ administration in jejunal cannulated rats.

The presented results are limited by the following factors. First, the liver PK inferred from various species is assumed to translate to human. Concerning liver bioavailability upon administration of the current tablet formulation at clinically relevant doses, our estimate is taken from the rat and dog studies, and it is uncertain how this will translate to human. Concerning liver half-life, it is likely that the translation is accurate, because similar estimates were obtained in dog and monkey and because monkey data were in agreement with a published PK model (15) as well as with estimated biophase half-lives for other ASOs targeting the liver (30). Second, there are no clinical studies that have assessed the administration of low doses of ASO at a once daily regimen and the consequences of this on target cell exposure. Geary *et al.* (31) and

Donner *et al.* (32) reported that a non-GalNAc-conjugated ASO administered as a subcutaneous bolus to mice resulted in similar liver exposure, but greater mRNA reduction, compared to an infusion of the same total dose. However, it can be expected that GalNAc-conjugated ASOs are less prone to such nonproductive uptake because they are taken up primarily by the ASGP receptor (12, 33), supported by the rat data presented here that indicate favorable target-engagement properties upon IJ administration. Third, although the dog and rat studies of the oral formulation were tested at clinically relevant doses, greater than therapeutically relevant doses were used in the monkey tolerability study. The emesis and abnormal feces at the two higher dose groups may have contributed to the variability of exposure to AZD8233. However, the saturated ASO exposure in the liver indicates that the compound was absorbed.

ASOs represent a therapeutic platform that can target genes encoding both intracellular and extracellular proteins. The technology is currently limited to parenteral administration. The presented data

therefore has broader implications for the platform. Oral delivery may become an option for development of other potent ASOs, especially for liver targets where GalNAc targeting can be exploited. This could also open up possibilities for fixed-dose combination products involving multiple ASOs or ASO combinations with orally delivered small molecules or peptides.

MATERIALS AND METHODS

Study design

The overall goal of the study was to investigate the feasibility of oral administration of AZD8233 coformulated in a tablet with sodium caprate as a transient permeation enhancer. The potency of AZD8233 was determined in transgenic mice ($N = 4$ per dose group) and humans ($N = 6$ per dose group) after subcutaneous administration. The target tissue half-life was investigated in monkeys ($N = 6$ to 12 per dose group) also after subcutaneous administration. Bioavailability after oral administration of AZD8233 formulated with sodium caprate was investigated in rats ($N = 4$ per dose group; IJ administration of a solution) and dogs ($N = 4$ to 10 per dose group; oral administration of tablets). Target engagement after oral administration was confirmed by IJ administration of a rat-specific surrogate ASO in solution with the enhancer to rats ($N = 4$ per dose group) and by plasma PCSK9 and LDL cholesterol lowering in cynomolgus monkeys after tablet administration ($N = 2$ per dose group).

Detailed information of compounds used in the studies is given in table S1. Table S5 summarizes the in vivo studies and their purposes. All animal studies were performed with humane care, and all protocols and procedures were approved by the respective country and institutional animal care and use committees.

Discovery of AZD8233 and potency in PCSK9 transgenic mice

A human cell-based transcriptomic analysis found no other transcripts reduced by AZD8233 across a range of concentration effective in reducing PCSK9 [≥ 10 -fold in median inhibitory concentration (IC_{50}) values for all transcripts compared to PCSK9]. Thus, AZD8233 is highly specific to reducing PCSK9 mRNA in human cells. The sequence of AZD8233 is the perfect complement to the cynomolgus PCSK9 sequence but not to the mouse sequence.

Human PCSK9 transgenic mice were generated by Ionis Pharmaceuticals. The genomic region of the human PCSK9 gene was excised from the appropriate fosmid, purified, and microinjected into fertilized oocytes. Oocytes were transferred to a pseudopregnant female, and pups were born. The pups were genotyped, and transgene-positive pups were checked for the expression of plasma PCSK9 protein. One animal was selected as a founder of the transgenic line and was transferred to Taconic Biosciences Inc. for breeding.

The objective of this study was to establish the PK and PD effects of AZD8233 after near steady-state dosing in transgenic mice with human PCSK9 expression (huPCSK9 Tg). Heterozygous 5-month-old, male huPCSK9 Tg mice were dosed with AZD8233 subcutaneously on days 1, 5, 8, 15, and 23 and euthanized on day 26 to quantify changes in human liver PCSK9 mRNA, human plasma PCSK9, and murine LDL cholesterol. Six dose groups (vehicle, 0.25, 0.5, 1, 2.5, and 5 mg/kg) with four animals in each group were used. At termination, plasma and liver tissue were collected for PK and PD measurement. Mice were housed as four per cage with each cage randomly selected into each of the six groups. Group sizes were calculated to detect up to 15% differences from vehicle control with a power of 80% and significance of 5%. Stopping criteria were based on animal welfare in line with our experimental animal license. All animals enrolled in the study completed the study, and all data obtained are reported in data file S1.

PCSK9 plasma protein concentrations in the PCSK9 transgenic mice were measured using a human PCSK9 enzyme-linked immunosorbent assay (ELISA) (R&D Systems, #DPC900). Murine LDL cholesterol was measured from the same plasma samples using the Olympus AU400e clinical analyzer with LDL cholesterol reagent (Beckman Coulter OSR6283). TaqMan quantitative reverse transcription polymerase chain reaction (RT-PCR) analysis was performed to evaluate liver PCSK9 expression in the PCSK9 transgenic mice. Values were normalized to total RNA measured by RiboGreen and report as percent difference versus control (Thermo Fisher Scientific).

The PCSK9 to liver exposure (Cliver) model was defined as: $PCSK9 = 100 \times (1 - \text{Cliver}^h / (\text{Cliver}^h + IC_{50}^h))$, where IC_{50} represents potency and h the Hill coefficient. Exposure of the vehicle group was assigned 0.1. The parameters were estimated as $IC_{50} = 2.0 \mu\text{g/g}$ (1.4 and 2.9 $\mu\text{g/g}$; 5th and 95th percentiles), $h = 2.2$ (1.6 and 3.8). Uncertainty of parameter estimates was determined by bootstrapping, sampling single measurements randomly with replacement within each dose group ($N = 1000$).

A similarly designed study was performed using the nonconjugated ION-848833 with five dose groups (vehicle, 1, 2.5, 5, and 10 mg/kg). The parameters were estimated as $IC_{50} = 16 \mu\text{g/g}$ (8.3 and 26 $\mu\text{g/g}$; 5th and 95th percentiles) and $h = 1.6$ (1.0 and 4.8).

Pcsk9 mouse study

The objective was to quantify endogenous PCSK9 knockdown effects using a hepatocyte-targeted GalNAc-conjugated murine Pcsk9 ASO on liver LDLR protein expression and lipoproteins lipid composition

in mice. Liver LDLR protein concentrations were measured with an ELISA, and lipid concentrations in different lipoprotein particles were measured after sequential D_2O /sucrose density ultracentrifugation separation of the lipoprotein classes. Group size justification and power analysis were performed on the basis of our previous experience with variability using the sequential D_2O /sucrose density ultracentrifugation methodology. Stopping criteria were based on animal welfare in line with our experimental animal license. All animals enrolled in the study completed the study, and all data obtained are reported in table S2 and in data file S2.

In total, 30 male C57BL/6J mice (Charles River) were housed in transparent polycarbonate cages containing hardwood bedding and nesting material. The mice had free access to water and standard chow diet (R70, Lantmännen) in an Association for Assessment and Accreditation of Laboratory Animal Care International-accredited facility with 12-hour light/dark cycle (lights on 6:00 a.m.), room temperature of 21° to 22°C, and relative humidity of 40 to 60%. At 10 weeks of age, mice were randomized into three study groups based on body weight and plasma triglyceride concentrations and then dosed once weekly with subcutaneous injections with either Pcsk9 ASO (IONIS-866672; $N = 10$), a control ASO (ION-740133; $N = 10$) at the dose of 5 mg/kg, or vehicle ($N = 10$) for 6 weeks. There were no differences in body weight change between the treatment groups. Before termination, the mice were fasted for 4 hours, blood was extracted from isoflurane (Forene, Abbot Scandinavia)-anesthetized mice, and plasma was isolated and frozen at -20°C . Livers were extracted and frozen at -80°C .

Liver and plasma triglycerides were determined as described before (34). Cholesterol in liver and plasma were analyzed with ABX Pentra Cholesterol CP (#A11A101634, Horiba Medical), using MultiCal as standard and P-Control (#A11A01654, Horiba Medical). Lipoproteins (VLDL, IDL, LDL, and HDL) were isolated from 100- μl plasma by sequential D_2O /sucrose density ultracentrifugation according to Ståhlman *et al.* (35). All isolated fractions analyzed for cholesterol and triglyceride concentrations were as described above. Phospholipids were analyzed using an assay from mti-diagnostics GmbH (#555-752) using Seronorm lipid (#100205, Sero AS) as control. Protein concentrations were analyzed using a Bio-Rad protein assay (#500-006); γ -globulin standard (#500-005, Bio-Rad) for VLDL, LDL, and IDL fractions; and bovine serum albumin (#500-007, Bio-Rad) for HDL fractions.

Plasma mouse PCSK9 protein concentrations were measured using a mouse PCSK9 ELISA (R&D Systems, #MPC900). Liver LDLR protein concentrations were measured using 40- to 60-mg liver tissues (homogenized in cell lysis buffer 2 from R&D Systems, #895347) using a mouse LDLR ELISA (R&D Systems, #MLDLR0).

Mouse liver triglyceride secretion study

The objective of this study was to determine whether PCSK9 inhibition affects liver triglyceride secretion. Six-week-old male C57BL/6J mice (the Jackson laboratory) were fed a high-fat diet (HFD) (TD88137, Envigo) for 1 week before ASO treatment. Mice were maintained on the HFD and treated ($N = 7$ per group) with saline, PCSK9 mAb (30 mg/kg), a mouse Pcsk9 ASO (ION-866672; 5 mg/kg per week), or microsomal triglyceride transfer protein (Mtp) ASO (ION-144477, 50 mg/kg per week) via once weekly subcutaneous injections for 3 weeks. Mtp ASO treatment was included as a positive control. Forty-eight hours after the final dose, mice were fasted for 4 hours, a baseline bleed was performed, and the mice were then intravenously

administered with 15% tyloxapol (Sigma-Aldrich) at a dose of 5 µl/g of body weight. Plasma time points were collected at 0, 0.5, 1, 2, and 3 hours. Time points were then analyzed for plasma triglycerides using a colorimetric assay. Stopping criteria were based on animal welfare in line with our experimental animal license. All animals enrolled in the study completed the study, and all data obtained are reported in data file S3.

Cynomolgus monkey study, subcutaneous injection

The objective of the study was to determine the potential toxicity of AZD8233 when given by subcutaneous injection to cynomolgus monkeys dosed on days 1, 8, 29, 57, and 85 with a minimum 3-month recovery period to evaluate the potential reversibility of any findings. Plasma and tissue samples were analyzed to assess exposure to AZD8233. The cynomolgus monkey is considered to be a pharmacologically relevant species because the AZD8233 sequence is the perfect complement to the monkey sequence. The total number of animals was considered to be the minimum required to properly characterize the effects of AZD8233. The study was designed such that it does not require an unnecessary number of animals to accomplish its objectives. Animals were randomly assigned to groups, and individual body weights were reviewed to ensure a balanced distribution was obtained. Animal welfare was controlled by the U.K. Home Office by the issue of licenses under the Animals (Scientific Procedures) Act 1986.

A 3-month study with subcutaneous injections was performed in male ($N = 19$) and female ($N = 19$) 2- to 3-year-old cynomolgus monkeys weighing 2 to 3 kg. A dose of 2 mg/kg ($N = 6$), 8 mg/kg ($N = 12$), or 32 mg/kg ($N = 10$), or vehicle ($N = 10$) was given on days 1, 8, 29, 57, and 85. In Fig. 6C, doses are expressed in milligrams per month and, hence, recalculated with average body weights for each arm. Termination occurred at different time points (Fig. 2). The study included a 3-month washout period at the highest dose. Liver tissues were collected for measurement of unconjugated AZD8233 concentrations by LC-MS/MS. LDL cholesterol was measured by an enzymatic colorimetric assay. One animal in the 8 mg/kg group with chronic treatment was terminated on day 22 due to animal welfare reasons. All other animals enrolled in the study completed the study, and all data obtained are reported in data file S4.

To estimate the tissue half-life, a one-compartment mathematical model with a dose-dependent volume of distribution was simultaneously fitted to data from all groups (Fig. 2). The absorption constant was fixed at 1 day⁻¹, volume of distribution = $V \times \text{dose}^\gamma$, with $V = 0.0524$ (0.044 and 0.062; 5th and 95th percentiles), and $\gamma = 0.178$ (0.11 and 0.25), dose in unit of milligram per kilogram, and elimination rate = 0.0394 day⁻¹ (0.033 and 0.045 day⁻¹). The nonlinearity with respect to dose on volume likely represent saturated liver uptake at high doses. Information about the half-life is obtained both from terminal sampling at steady state and from time series sampling of the terminal phase during washout. The accumulation, α , for once daily dosing was calculated as $\alpha = 1/[1 - \exp(-\tau \times \log(2)/t_{\text{half}})]$ where τ represents the time between doses (here, $\tau = 1$ day).

Clinical study, subcutaneous injection

The study (NCT03593785) was conducted with the aim to evaluate the safety and tolerability of single escalating subcutaneous doses of AZD8233 in a small number of subjects before proceeding to repeated subcutaneous dosing and larger number of patient studies. Secondary objectives were to assess the effect of AZD8233 in reducing

the concentrations of PCSK9, LDL cholesterol, and other lipid biomarker in plasma and to characterize the PK of AZD8233. The study was not powered for evaluation of efficacy or the degree of reduction in PCSK9 or lipid biomarkers. Subjects were randomized to receive treatment with AZD8233 or placebo in a ratio of 6:2 per dose cohort. The study was single blind. The study participants were blinded during the entire study, and personnel at the study site were blinded during the study. Study sponsor personnel with exception of personnel evaluating PK were also blinded up to the safety review committee meeting. In each cohort, blood samples for analysis of PCSK9 in plasma was collected at screening; the day before dosing and only before dosing; 24 and 72 hours after dosing; and thereafter at 1, 2, 3, 4, 6, 8, 10, 12, and 16 weeks after dose. The study was conducted at the Parexel Early Phase Clinical Unit in Los Angeles, and the study protocol was approved by the Local Ethics Committee. All subjects completed the study, and all data obtained are reported in data file S5.

The study was conducted in healthy male subjects with elevated LDL cholesterol (100 to <190 mg/dl) and with weight and age ranging between 63 and 101 kg and 19 and 58 years, respectively. PCSK9 concentrations were measured with an ELISA method (DPC900, R&D Systems), capturing the total concentrations of PCSK9 in plasma. LDL cholesterol was measured with an enzymatic colorimetric assay (Roche).

Rat study

The objective was to separately investigate the dose-dependent tissue exposure of AZD8233 targeting human PCSK9 (but inactive in the rat) and ION-704361 targeting rat *Malat-1* for single-dose IJ and subcutaneous administration, as well as the bioavailabilities of two ASOs for IJ compared to subcutaneous administration. A secondary objective was to quantify target engagement in the form of *Malat-1* mRNA expression and knockdown. The two ASOs have similar chemistry: 16-nucleotide oligomer cEt modified and GalNAc conjugated.

Male Sprague-Dawley rats, 6 to 8 weeks and weighing 200 to 250 g, with surgically implanted IJ catheter were exposed to ION-704361 or AZD8233, using a single IJ dose, with $N = 4$ per group. For subcutaneous administration, the same design was used but using non-catheterized rats. The sample size was justified on the basis of previous experience of PK studies with IJ administration (36). Rats were randomized into five dose groups per dosing route and per compound for bioavailability evaluation. Stopping criteria were based on animal welfare in line with our experimental animal license. All animals enrolled in the study completed the study, and all data obtained are reported in data file S6.

The liver bioavailability in IJ cannulated rats was quantified after both IJ and subcutaneous single-dose administration (IJ doses of 0, 3, 10, 20, and 40 mg/kg together with sodium caprate at 300 mg/kg as permeation enhancer; subcutaneous doses of 0, 0.3, 1, 2, and 4 mg/kg without permeation enhancer). All animals were euthanized at 48 hours after dose. Plasma, liver, and kidney were collected at 48 hours. Hybridization ELISA was performed for plasma and LC-MS/MS analysis for tissue ASO concentration analysis. ION-863633 and ION-704361 plasma lower limit of quantification (LLOQ) was 0.15 nM. Unconjugated AZD8233 and ION-704361 tissue LLOQ were 0.054 and 0.0269 µg/g, respectively. *Malat-1* mRNA expression and knockdown in liver and intestine were also assessed by real-time PCR, and relative concentrations with respect to the subcutaneous control group were reported.

Dog study

The objective of the study was to evaluate the liver and plasma bio-availability after oral versus subcutaneous dosing and to determine the potential toxicity of AZD8233 when given for 28 days to beagle dogs. Plasma and tissues samples were analyzed to assess exposure to AZD8233. The total number of animals was considered to be the minimum required to properly characterize the effects of AZD8233; hence, the study was designed not to require an unnecessary number of animals to accomplish its objectives. Animals were randomly assigned to groups on the basis of body weight. The study plan was reviewed and approved by CR-SHB the Institutional Animal Care and Use Committee of Charles River Laboratories. During the study, the care and use of animals was conducted with guidance from the U.S. National Research Council and the Canadian Council on Animal Care. All animals enrolled in the study completed the study, and all data obtained are reported in data file S7.

AZD8233 was daily dosed to 19 male beagle dogs (body weight of 6.9 to 9.3 kg at the start of the study) as an oral enteric-coated tablet containing 3 or 20 mg of AZD8233 together with 700 mg of sodium caprate as permeation enhancer or as an SC solution (1 mg/ml) for 7 or 28 days. The oral doses were 3 mg/day ($N = 5$) or 20 mg/day ($N = 10$), where half of the high-dose animals were terminated after 7 days of dosing. The SC dose was 1 mg/day ($N = 4$), and half of these animals were also terminated after 7 days of dosing. Thirty minutes or less before tablet administration, a solution of 0.1 M HCl/KCl was administered by oral gavage to ensure acidic conditions in the stomach. To facilitate swallowing, the tablet was placed as far back into the throat as possible followed by a tap water flush (10 ml). The SC dose was injected into the scapular and mid-dorsal areas. The plasma exposure was evaluated on days 1, 7, and 28 by taking blood samples from the jugular vein up to 24 hours after dose. In addition, liver, kidney, and jejunum tissue samples were taken at necropsy and concentrations of unconjugated AZD8233 were measured. The following parameters were assessed: detailed clinical observations, body weights, food consumption, hematology, coagulation, clinical chemistry, organ weights, and gross and microscopic pathology. The following tissues were examined microscopically: kidney, liver, injection site (only SC arm), stomach, duodenum, jejunum, ileum, caecum, colon, and rectum. LLOQ for tissue samples: 0.500 $\mu\text{g/g}$ (kidney and jejunum), 1.04 $\mu\text{g/g}$ (AZD6615 liver), and 0.810 $\mu\text{g/g}$ (unconjugated AZD6615 liver). Plasma LLOQ = 0.0346 ng/ml. In the model fit to data, the estimated σ^2 was 0.0997 $\mu\text{g/g} \times \mu\text{g/g}$ (0.030 and 0.14 $\mu\text{g/g} \times \mu\text{g/g}$; 5th and 95th percentiles).

Cynomolgus monkey study, oral tablet administration

The objective of the study was to determine the potential tolerability of AZD8233, when given oral tablet once daily for 14 days, to cynomolgus monkeys. Plasma samples were analyzed to assess exposure to AZD8233. The cynomolgus monkey was chosen as the animal model for this study because it is an accepted nonrodent species for preclinical toxicity testing by regulatory agencies. The total number of animals was considered to be the minimum required to properly characterize the effects of AZD8233. The study was designed such that it does not require an unnecessary number of animals to accomplish its objective. Animal welfare was controlled by the U.K. Home Office by the issue of licenses under the Animals (Scientific Procedures) Act 1986. All subjects completed the study, and all data obtained are reported in data file S8.

Three groups each consisting of one male and one female cynomolgus monkey (body weight of 2.5 to 3.1 kg at day 1) were given AZD8233 formulated in an enteric-coated tablet with sodium caprate (14-mg AZD8233 and 500-mg sodium caprate) by daily oral tablet administration for 14 days at dose levels of two, three, or four tablets per day. The doses were given using a syringe with attached gavage tubing: The tablet was placed into the end of the gavage and expelled from the gavage using a syringe containing water. The following parameters were assessed: clinical observations, body weights, hematology, plasma chemistry, PCSK9 protein concentrations, concentrations of AZD8233 in plasma and tissue, organ weights, and gross and microscopic pathology. Samples for microscopic evaluation were collected 24 hours after the last dose. The following tissues were examined microscopically: adrenal gland, bone marrow, bone, brain, eye, heart, kidney, liver, lung, pancreas, small intestine (duodenum, jejunum, and ileum), spleen, stomach, testis, and thymus. Liver exposure was measured by LC-MS/MS; plasma PCSK9 by ELISA; and LDL cholesterol, cholesterol, and triglycerides by enzymatic colorimetric assays.

ASO exposure analysis in plasma and tissue

For plasma analysis of ASOs, a dual-probe hybridization assay using electrochemiluminescence was used on the MSD platform (Meso Scale Discovery). Briefly, a biotinylated capture probe was mixed with the sample and heated to 80°C and mixed for 60 min at 500 rpm. The samples were allowed to cool to room temperature, and then the mixture was added to preblocked MSD streptavidin plates (Meso Scale Discovery) and incubated for 30 min at room temperature. The plates were washed three times with tris-buffered saline and tween 20 (TBS-T). Preheated (65°C) Sulfo-TAG-labeled detector probe was added to the plates and incubated for 60 min at room temperature in the dark. The plates were washed three times with TBS-T, one-time MSD read buffer was added to the wells, and the plates were read within 5 min on an MSD Sector reader.

Tissue samples analyzed for ION-704361 with LC-MS were homogenized in $\text{H}_2\text{O}:\text{NH}_4\text{OH}$ (2:1) using a bead beater system. The homogenates and plasma samples (100 μl) were extracted using liquid-liquid extraction with phenol-chloroform-isoamyl alcohol (Sigma-Aldrich). The water phase was collected and dried under N_2 , resuspended in H_2O , and analyzed with LC coupled to a triple quadrupole MS (LC-MS/MS). The MS was operated in negative mode, the precursor ion mass was set to the most abundant charge state of the ASO, and the product ion mass was set to the phosphorothioate backbone fragment mass/charge ratio of 95. The LC was equipped with a 50-mm C18 analytical column and used with ion pairing mobile phases.

Tissue concentrations for AZD8233 were determined using ion-pairing ultra-performance LC with MS/MS (LC-MS/MS) after tissue homogenization, liquid-liquid extraction, and solid-phase extraction procedures, similar to ION-704361. A 27-nucleotide oligomer oligonucleotide was added before extraction as internal standard.

Human PKPD model

Prediction of human PKPD was made using a mathematical model built upon liver PK data from cynomolgus monkey, potency data from transgenic mouse, and literature data on plasma PCSK9 and LDL cholesterol dynamics. Previously, at least qualitatively, translation of a liver exposure-PCSK9 relationship has been demonstrated between transgenic mouse, cynomolgus monkey, and human for an siRNA PCSK9 inhibitor upon SC administration (37, 38).

The dose to liver exposure model was taken from the SC monkey study. To avoid extrapolation of the nonlinearity on dose, the lowest dose of 2 mg/kg in the monkey study was used in the expression for volume of distribution. A human body weight of 80 kg was assumed in the simulation.

The liver exposure–PCSK9 model was defined as a turnover model $PCSK9'(t) = k_{in} \times (1 - Cliver^h / (Cliver^h + IC_{50}^h)) - k_{out} \times PCSK9(t)$, where $IC_{50} = 2.0$ $\mu\text{g/g}$ and the Hill coefficient $h = 2.2$ were taken from the AZD8233-exposed transgenic mouse model and where $k_{in} = R_0 \times k_{out}$ with $R_0 = 100$. The parameter k_{out} was inferred from literature data as described next.

The PCSK9–LDL cholesterol model was based on inclisiran data (39), which were digitized, and modeled by an empirical PKPD model similar to previously described (fig. S5) (30). The apparent PK was modeled by a one-compartment model with linear elimination, having parameters $k_a = 0.139$ day^{-1} (0.11 and 0.16 day^{-1} ; 5th and 95th percentiles), $V = 1$ (fixed), and $k_e = 0.00846$ day^{-1} (0.0078 and 0.0092 day^{-1}). Plasma PCSK9 was modeled by a turnover model with inhibition of production and driven by the apparent PK, having parameters $R_0 = 1$ (fixed), $k_{out} = 0.188$ day^{-1} (0.17 and 0.21 day^{-1}), $I_{max} = 1$ (fixed), $IC_{50} = 50.8$ (45 and 56), and $h = 0.603$ (0.56 and 0.65). LDL cholesterol was modeled by a turnover model with activation of loss by plasma PCSK9 decrease: $LDL\ cholesterol'(t) = k_{in2} - k_{out2} \times (1 + A \times PCSK9_{decrease}(t)^{h_2}) \times LDL\ cholesterol(t)$, where $PCSK9_{decrease}(t) = 1 - PCSK9(t)$ and $k_{in2} = k_{out2} \times LDL\ cholesterol(0)$. The parameters were inferred as LDL cholesterol(0) = 1 (fixed), $k_{out2} = 0.251$ day^{-1} (0.20 and 0.31 day^{-1}), $A = 2.06$ (1.9 and 2.3), and $h_2 = 2.22$ (2.0 and 2.4).

Parameter estimation

Parameter estimation was performed according to a maximum likelihood approach with a multiplicative lognormal error model for PK models, and an additive error model for PD models, using the naive-pooled data approach. Uncertainty of parameter estimates was determined by bootstrapping, sampling single measurements randomly with replacement within each experiment ($N = 500$). Numeric analyses were performed in MATLAB (R2019b; MathWorks). Specifically, the MATLAB function `fminsearch` was used for solving the optimization problems encountered during parameter estimation.

Statistical analysis

Normality of data was investigated using the one-sample Kolmogorov–Smirnov test. For data of the transgenic mouse study (Fig. 1), log-transformed data were suggested for plasma PCSK9, and normal scale for other variables. For data of the rat study (Fig. 4 and table S3), log-transformed data were suggested for *Malat-1* mRNA expression. Tukey's post hoc test was used for multiple comparisons. Calculations were performed in MATLAB. Specifically, the function `kstest` was used to test for normality, and the functions `anova1` and `multcompare` were used for multiple comparison tests. Statistics of table S2 was performed using GraphPad Prism version 8.0.0 for Windows, GraphPad Software; www.graphpad.com.

SUPPLEMENTARY MATERIALS

stm.sciencemag.org/cgi/content/full/13/593/eabe9117/DC1

Fig. S1. Chemical structure of AZD8233 as sodium salt.

Fig. S2. The non–GalNAc-conjugated parent of AZD8233, ION 848833, in a 4-week dose-response study in transgenic mouse overexpressing human PCSK9.

Fig. S3. Pcsk9 GalNAc ASO treatment did not reduce liver triglyceride secretion in wild-type mice fed with an HFD.

Fig. S4. Plasma concentration after repeated daily oral administration of AZD8233 tablets to dogs.

Fig. S5. Empirical PKPD model of PCSK9 and LDL cholesterol.

Table S1. Information about compounds used in the studies.

Table S2. Effects of 6-week subcutaneous administration (5 mg/kg, once weekly) of mouse Pcsk9 ASO, control ASO, or vehicle in C57BL/6J male mice on plasma Pcsk9 protein concentrations, liver LDL protein expression, and plasma and liver lipid concentrations.

Table S3. Knockdown of *Malat-1* mRNA in liver and intestine after a single dose of rat-specific GalNAc-conjugated tool ASO targeting *Malat-1* (ION-704361) with sodium caprate (300 mg/kg) as permeation enhancer after IJ administration to rats.

Table S4. LDL cholesterol, total cholesterol, triglycerides, and concentration of unconjugated AZD8233 in the liver in the 14-day tolerability study in monkeys.

Table S5. Overview of animal studies and their purposes.

Data file S1. Transgenic mouse, Fig. 1 and fig. S2.

Data file S2. Wild-type mouse Pcsk9 and lipid concentrations, table S2.

Data file S3. Wild-type mouse triglyceride secretion, fig. S3.

Data file S4. Monkey PK, Fig. 2.

Data file S5. Human PCSK9 and LDL cholesterol, Fig. 3.

Data file S6. Rat PK and knockdown, Fig. 4 and table S3.

Data file S7. Dog PK, Fig. 5 and fig. S4.

Data file S8. Monkey PCSK9 and LDL cholesterol, Fig. 6.

[View/request a protocol for this paper from Bio-protocol.](#)

REFERENCES AND NOTES

- C. N. Hess, C. C. Low Wang, W. R. Hiatt, PCSK9 inhibitors: Mechanisms of action, metabolic effects, and clinical outcomes. *Annu. Rev. Med.* **69**, 133–145 (2018).
- P. El Khoury, S. Elbittar, Y. Ghaleb, Y. A. Khalil, M. Varret, C. Boileau, M. Abifadel, PCSK9 mutations in familial hypercholesterolemia: From a groundbreaking discovery to anti-PCSK9 therapies. *Curr. Atheroscler. Rep.* **19**, 49 (2017).
- J. C. Cohen, E. Boerwinkle, T. H. Mosley Jr., H. H. Hobbs, Sequence variations in PCSK9, low LDL, and protection against coronary heart disease. *N. Engl. J. Med.* **354**, 1264–1272 (2006).
- M. S. Sabatine, R. P. Giugliano, S. D. Wiviott, F. J. Raal, D. J. Blom, J. Robinson, C. M. Ballantyne, R. Somaratne, J. Legg, S. M. Wasserman, R. Scott, M. J. Koren, E. A. Stein; Open-Label Study of Long-Term Evaluation against LDL Cholesterol (OSLER) Investigators, Efficacy and safety of evolocumab in reducing lipids and cardiovascular events. *N. Engl. J. Med.* **372**, 1500–1509 (2015).
- E. M. Roth, P. M. Moriarty, J. Bergeron, G. Langslet, G. Manvelian, J. Zhao, M. T. Baccara-Dinet, D. J. Rader; ODYSSEY CHOICE I investigators, A phase III randomized trial evaluating alirocumab 300 mg every 4 weeks as monotherapy or add-on to statin: ODYSSEY CHOICE I. *Atherosclerosis* **254**, 254–262 (2016).
- M. S. Sabatine, PCSK9 inhibitors: Clinical evidence and implementation. *Nat. Rev. Cardiol.* **16**, 155–165 (2018).
- F. J. Raal, R. Chilton, N. Ranjith, V. Rambiritch, R. F. Leisegang, I. O. Ebrahim, A. V. Tonder, N. Shunmugam, C. Bouharati, M. G. Musa, S. Karamchand, P. Naidoo, D. J. Blom, PCSK9 inhibitors: From nature's lessons to clinical utility. *Endocr. Metab. Immune Disord. Drug Targets* **20**, 840–854 (2020).
- F. J. Raal, D. Kallend, K. K. Ray, T. Turner, W. Koenig, R. S. Wright, P. L. J. Wijngaard, D. Curcio, M. J. Jaros, L. A. Leiter, J. J. P. Kastelein; ORION-9 Investigators, Inclisiran for the treatment of heterozygous familial hypercholesterolemia. *N. Engl. J. Med.* **382**, 1520–1530 (2020).
- K. K. Ray, R. S. Wright, D. Kallend, W. Koenig, L. A. Leiter, F. J. Raal, J. A. Bischoff, T. Richardson, M. Jaros, P. L. J. Wijngaard, J. J. P. Kastelein; ORION-10 and ORION-11 Investigators, Two phase 3 trials of inclisiran in patients with elevated LDL cholesterol. *N. Engl. J. Med.* **382**, 1507–1519 (2020).
- B. G. Nordestgaard, S. J. Nicholls, A. Langsted, K. K. Ray, A. Tybjaerg-Hansen, Advances in lipid-lowering therapy through gene-silencing technologies. *Nat. Rev. Cardiol.* **15**, 261–272 (2018).
- E. A. Biessen, H. Vietsch, E. T. Rump, K. Fluiter, J. Kuiper, M. K. Bijsterbosch, T. J. van Berkel, Targeted delivery of oligodeoxynucleotides to parenchymal liver cells in vivo. *Biochem. J.* **340** (3), 783–792 (1999).
- T. P. Prakash, M. J. Graham, J. Yu, R. Carty, A. Low, A. Chappell, K. Schmidt, C. Zhao, M. Aghajan, H. F. Murray, S. Riney, S. L. Booten, S. F. Murray, H. Gaus, J. Crosby, W. F. Lima, S. Guo, B. P. Monia, E. E. Swayze, P. P. Seth, Targeted delivery of antisense oligonucleotides to hepatocytes using triantennary *N*-acetyl galactosamine improves potency 10-fold in mice. *Nucleic Acids Res.* **42**, 8796–8807 (2014).
- M. J. Graham, R. G. Lee, T. A. Brandt, L. J. Tai, W. Fu, R. Peralta, R. Yu, E. Hurh, E. Paz, B. W. McEvoy, B. F. Baker, N. C. Pham, A. Digenio, S. G. Hughes, R. S. Geary, J. L. Witztum, R. M. Crooke, S. Tsimikas, Cardiovascular and metabolic effects of ANGPTL3 antisense oligonucleotides. *N. Engl. J. Med.* **377**, 222–232 (2017).
- S. T. Crooke, B. F. Baker, S. Xia, R. Z. Yu, N. J. Viney, Y. Wang, S. Tsimikas, R. S. Geary, Integrated assessment of the clinical performance of GalNAc₃-conjugated 2'-O-methoxyethyl chimeric

- antisense oligonucleotides: I. Human volunteer experience. *Nucleic Acid Ther.* **29**, 16–32 (2019).
15. R. Z. Yu, R. Gunawan, N. Post, T. Zanardi, S. Hall, J. Burkey, T. W. Kim, M. J. Graham, T. P. Prakash, P. P. Seth, E. E. Swayze, R. S. Geary, S. P. Henry, Y. Wang, Disposition and pharmacokinetics of a GalNAC3-conjugated antisense oligonucleotide targeting human lipoprotein (a) in monkeys. *Nucleic Acid Ther.* **26**, 372–380 (2016).
 16. S. Maher, D. J. Brayden, L. Casettari, L. Illum, Application of permeation enhancers in oral delivery of macromolecules: An update. *Pharmaceutics* **11**, 41 (2019).
 17. S. T. Crooke, X.-H. Liang, R. M. Crooke, B. F. Baker, R. S. Geary, Antisense drug discovery and development technology considered in a pharmacological context. *Biochem. Pharmacol.* **114**, 196 (2020).
 18. L. G. Tillman, R. S. Geary, G. E. Hardee, Oral delivery of antisense oligonucleotides in man. *J. Pharm. Sci.* **97**, 225–236 (2008).
 19. R. M. Stoekenbroek, G. Lambert, B. Cariou, K. G. Hovingh, Inhibiting PCSK9 — Biology beyond LDL control. *Nat. Rev. Endocrinol.* **15**, 52–62 (2018).
 20. B. Davies, T. Morris, Physiological parameters in laboratory animals and humans. *Pharm. Res.* **10**, 1093–1095 (1993).
 21. S. T. Crooke, J. L. Witzum, C. F. Bennett, B. F. Baker, RNA-targeted therapeutics. *Cell Metab.* **27**, 714–739 (2018).
 22. A. Khvorova, J. K. Watts, The chemical evolution of oligonucleotide therapies of clinical utility. *Nat. Biotechnol.* **35**, 238–248 (2017).
 23. Y. Wang, R. Z. Yu, S. Henry, R. S. Geary, Pharmacokinetics and clinical pharmacology considerations of GalNAC₃-conjugated antisense oligonucleotides. *Expert Opin. Drug Metab. Toxicol.* **15**, 475–485 (2019).
 24. V. Sokolov, G. Helmlinger, C. Nilsson, K. Zhudnikov, S. Skrtic, B. Hamren, K. Peskov, E. Hurt-Camejo, R. Jansson-Löfmark, Comparative quantitative systems pharmacology modeling of anti-PCSK9 therapeutic modalities in hypercholesterolemia. *J. Lipid Res.* **60**, 1610–1621 (2019).
 25. R. S. Geary, R. Z. Yu, T. Watanabe, S. P. Henry, G. E. Hardee, A. Chappell, J. Matson, H. Sasnor, L. Cummins, A. A. Levin, Pharmacokinetics of a tumor necrosis factor- α phosphorothioate 2'-O-(2-methoxyethyl) modified antisense oligonucleotide: Comparison across species. *Drug Metab. Dispos.* **31**, 1419–1428 (2003).
 26. C. Granhall, M. Donsmark, T. M. Blicher, G. Golor, F. L. Sondergaard, M. Thomsen, T. A. Bækdal, Safety and pharmacokinetics of single and multiple ascending doses of the novel oral human GLP-1 analogue, oral semaglutide, in healthy subjects and subjects with type 2 diabetes. *Clin. Pharmacokinet.* **58**, 781–791 (2019).
 27. C. Twarog, S. Fattah, J. Heade, S. Maher, E. Fattal, D. J. Brayden, Intestinal permeation enhancers for oral delivery of macromolecules: A comparison between salcaprozate sodium (SNAC) and sodium caprate (C₁₀). *Pharmaceutics* **11**, 78 (2019).
 28. B. Shi, M. Abrams, L. Sepp-Lorenzino, Expression of asialoglycoprotein receptor 1 in human hepatocellular carcinoma. *J. Histochem. Cytochem.* **61**, 901–909 (2013).
 29. J. Scharner, S. Qi, F. Rigo, C. F. Bennett, A. R. Krainer, Delivery of GalNAC-conjugated splice-switching ASOs to non-hepatic cells through ectopic expression of asialoglycoprotein receptor. *Mol. Ther. Nucleic Acids* **16**, 313–325 (2019).
 30. R. Jansson-Löfmark, P. Gennemark, Inferring half-lives at the effect site of oligonucleotide drugs. *Nucleic Acid Ther.* **28**, 319–325 (2018).
 31. R. S. Geary, E. Wanciewicz, J. Matson, M. Pearce, A. Siwkowski, E. Swayze, F. Bennett, Effect of dose and plasma concentration on liver uptake and pharmacologic activity of a 2'-methoxyethyl modified chimeric antisense oligonucleotide targeting PTEN. *Biochem. Pharmacol.* **78**, 284–291 (2009).
 32. A. J. Donner, E. V. Wanciewicz, H. M. Murray, S. Greenlee, N. Post, M. Bell, W. F. Lima, E. E. Swayze, P. P. Seth, Co-administration of an excipient oligonucleotide helps delineate pathways of productive and nonproductive uptake of phosphorothioate antisense oligonucleotides in the liver. *Nucleic Acid Ther.* **27**, 209–220 (2017).
 33. S. T. Crooke, S. Wang, T. A. Vickers, W. Shen, X. H. Liang, Cellular uptake and trafficking of antisense oligonucleotides. *Nat. Biotechnol.* **35**, 230–237 (2017).
 34. D. Lindén, A. Ahnmark, P. Pingitore, E. Ciociola, I. Ahlstedt, A.-C. Andréasson, K. Sasidharan, K. Madeyski-Bengtson, M. Zurek, R. M. Mancina, A. Lindblom, M. Bjursell, G. Böttcher, M. Ståhlman, M. Bohlooly-Y, W. G. Haynes, B. Carlsson, M. Graham, R. Lee, S. Murray, L. Valenti, S. Bhanot, P. Åkerblad, S. Romeo, Pnpla3 silencing with antisense oligonucleotides ameliorates nonalcoholic steatohepatitis and fibrosis in *Pnpla3* I148M knock-in mice. *Mol. Metab.* **22**, 49–61 (2019).
 35. M. Ståhlman, P. Davidsson, I. Kanmert, B. Rosengren, J. Borén, B. Fagerberg, G. Camejo, Proteomics and lipids of lipoproteins isolated at low salt concentrations in D2O/sucrose or in KBr. *J. Lipid Res.* **49**, 481–490 (2008).
 36. S. Crooke, *Antisense Drug Technology Principles, Strategies, and Applications* (CRC Press, ed. 2, 2007).
 37. M. Frank-Kamenetsky, A. Grefhorst, N. N. Anderson, T. S. Racie, B. Bramlage, A. Akinc, D. Butler, K. Charisse, R. Dorkin, Y. Fan, C. Gamba-Vitalo, P. Hadwiger, M. Jayaraman, M. John, K. N. Jayaprakash, M. Maier, L. Nechev, K. G. Rajeev, T. Read, I. Röhl, J. Soutschek, P. Tan, J. Wong, G. Wang, T. Zimmermann, A. de Fougerolles, H.-P. Vornlocher, R. Langer, D. G. Anderson, M. Manoharan, V. Kotliansky, J. D. Horton, K. Fitzgerald, Therapeutic RNAi targeting PCSK9 acutely lowers plasma cholesterol in rodents and LDL cholesterol in nonhuman primates. *Proc. Natl. Acad. Sci. U.S.A.* **105**, 11915–11920 (2008).
 38. K. Fitzgerald, M. Frank-Kamenetsky, S. Shulga-Morskaya, A. Liebow, B. R. Bettencourt, J. E. Sutherland, R. M. Hutabarat, V. A. Clausen, V. Karsten, J. Cehelsky, S. V. Nochur, V. Kotlianski, J. Horton, T. Mant, J. Chiesa, J. Ritter, M. Munisamy, A. K. Vaishnaw, J. A. Gollob, A. Simon, Effect of an RNA interference drug on the synthesis of proprotein convertase subtilisin/kexin type 9 (PCSK9) and the concentration of serum LDL cholesterol in healthy volunteers: A randomised, single-blind, placebo-controlled, phase 1 trial. *Lancet* **383**, 60, –68 (2014).
 39. K. K. Ray, U. Landmesser, L. A. Leiter, D. Kallend, R. Dufour, M. Karakas, T. Hall, R. P. Troquay, T. Turner, F. L. J. Visseren, P. Wijngaard, R. S. Wright, J. J. P. Kastelein, Inclisiran in patients at high cardiovascular risk with elevated LDL cholesterol. *N. Engl. J. Med.* **376**, 1430–1440 (2017).

Acknowledgments: We thank L. Aasehaug at the Research and Early Development Cardiovascular, Renal and Metabolism, and Animal Science and Technology, BioPharmaceuticals R&D, AstraZeneca, Gothenburg, Sweden for excellent technical assistance; M. Graham, Ionis Pharmaceuticals Inc., Carlsbad, California; and D. Han, Parexel, Glendale, California. **Funding:** There is no other funding than from the involved companies AstraZeneca and Ionis Pharmaceuticals. **Author contributions:** K.W., N.C., A.T., and N.D.: Designed and developed the oral formulation. M.H. and C.S.J.R.: Developed the bioanalytical method and analyzed samples. P.G., R.J.-L., U.A., M.E., Y.W., and R.Z.Y.: Design and interpretation of rat, monkey, and dog studies. S.J.R.: Acquisition, analysis, and interpretation of the preclinical transgenic data. D.L. and E.H.-C.: Manuscript editing, Pcsk9 mouse study design, and data interpretation. B.R. and D.K.-P.: Performed the Pcsk9 mouse study. D.R., C.A.M.N., J.K., L.W., and B.C.: Design and analysis of the clinical study. L.T.: Advice, experimental design, and data interpretation for oral formulation activities. R.I.: Statistics. R.C.: Design and interpretation of the preclinical transgenic experimental data and manuscript editing. R.S.G., B.P.M., T.R.-B., E.H.-C., B.C., M.E., A.T., and N.D.: Project conception, study design oversight, experimental data interpretation, and manuscript editing. P.G.: Drafted the manuscript and mathematical modeling. **Competing interests:** AstraZeneca filed a patent application (63/079,941) with inventors A.T., N.D., M.E., P.G., N.C., K.W., and L.T. directed to the subject matter disclosed in this manuscript. The patent application is a priority provisional application that is not publicly accessible. P.G., K.W., N.C., D.R., C.A.M.N., J.K., M.H., L.W., B.R., D.K.-P., R.I., R.J.-L., C.S.J.R., D.L., E.H.-C., T.R.-B., B.C., U.A., M.E., A.T., and N.D. are employees of AstraZeneca. B.P.M., R.S.G., R.Z.Y., Y.W., S.J.R., R.C., and L.T. are employed by Ionis. **Data and materials availability:** All data associated with this study are present in the paper or the Supplementary Materials. Antisense oligonucleotides associated with this study can be made available, upon reasonable request, to academic researchers under a material transfer agreement with AstraZeneca and Ionis Pharmaceuticals.

Submitted 9 October 2020

Accepted 23 April 2021

Published 12 May 2021

10.1126/scitranslmed.abe9117

Citation: P. Gennemark, K. Walter, N. Clemmensen, D. Rekić, C. A. Nilsson, J. Knöchel, M. Hølttä, L. Wernevik, B. Rosengren, D. Kakol-Palm, Y. Wang, R. Z. Yu, R. S. Geary, S. J. Riney, B. P. Monia, R. Isaksson, R. Jansson-Löfmark, C. S. J. Rocha, D. Lindén, E. Hurt-Camejo, R. Crooke, L. Tillman, T. Rydén-Bergsten, B. Carlsson, U. Andersson, M. Elebring, A. Tivesten, N. Davies, An oral antisense oligonucleotide for PCSK9 inhibition. *Sci. Transl. Med.* **13**, eabe9117 (2021).

An oral antisense oligonucleotide for PCSK9 inhibition

Peter Gennemark, Katrin Walter, Niclas Clemmensen, Dinko Reki, Catarina A.M. Nilsson, Jane Knchel, Mikko Hltt, Linda Wernevik, Birgitta Rosengren, Dorota Kakol-Palm, Yanfeng Wang, Rosie Z. Yu, Richard S. Geary, Stan J. Riney, Brett P. Monia, Rikard Isaksson, Rasmus Jansson-Lfmark, Cristina S. J. Rocha, Daniel Lindn, Eva Hurt-Camejo, Rosanne Crooke, Lloyd Tillman, Tina Rydn-Bergsten, Bjrn Carlsson, Ulf Andersson, Marie Elebring, Anna Tivesten, and Nigel Davies

Sci. Transl. Med., **13** (593), eabe9117.
DOI: 10.1126/scitranslmed.abe9117

An oral ASO to lower LDL

Strategies to decrease low-density lipoprotein (LDL) cholesterol could help treat atherosclerosis. Here, Gennemark *et al.* developed an antisense oligonucleotide (ASO) that can be delivered orally, is taken up by the liver, and targets PCSK9, which regulates the LDL receptor. Subcutaneous administration of the ASO showed high potency in mice overexpressing PCSK9, a liver half-life of 18 days in monkeys, and reduced circulating PCSK9 in humans. The oral formulation showed 5 to 7% liver bioavailability compared to subcutaneous administration in rats and dogs, and it reduced LDL cholesterol in healthy monkeys. Results support the potential of this ASO for PCSK9 inhibition while avoiding the need for injections.

View the article online

<https://www.science.org/doi/10.1126/scitranslmed.abe9117>

Permissions

<https://www.science.org/help/reprints-and-permissions>

Use of this article is subject to the [Terms of service](#)